Unusual Low-Energy Phonon Dynamics in the Negative Thermal Expansion Compound ZrW_2O_8

Jason N. Hancock, Chandra Turpen, and Zack Schlesinger
Physics Department, University of California–Santa Cruz, Santa Cruz, California 95064, USA

Glen R. Kowach
Department of Chemistry, The City College of New York, New York, New York 10031, USA

Arthur P. Ramirez
Bell Laboratories, Lucent Technologies, 600 Mountain Avenue, Murray Hill, New Jersey 07974, USA

(Received 10 August 2004; published 22 November 2004)

An infrared study of the phonon spectra of ZrW_2O_8 as a function of temperature which includes the low-energy (2–10 meV) region relevant to negative thermal expansion is reported and discussed in the context of specific heat and neutron density of state results. The prevalence of infrared active phonons at low energy and their observed temperature dependence are highly unusual and indicative of exotic low-energy lattice dynamics. Eigenvector calculations indicate a mixing of librational and translational motion within each low-frequency IR mode. The role of the underconstrained structure in establishing the nature of these modes and the relationship between the IR spectra and the large negative thermal expansion in ZrW_2O_8 are discussed.

DOI: 10.1103/PhysRevLett.93.225501 PACS numbers: 63.20.–e, 65.40.De, 78.30.–j

The tendency of solids to expand when heated is one of the most pervasive and familiar phenomena in solid state physics [1]; however, there are some compounds in which the opposite phenomenon occurs [2,3]. In ZrW_2O_8 this negative thermal expansion (NTE) is large, isotropic, and persists over a broad temperature range [4–9]. These characteristics enhance our interest in both the fundamental physics of ZrW_2O_8, and the potential applications of such a substantial NTE effect, which are widespread [3]. A defining feature of ZrW_2O_8 is the existence of a onefold coordinated oxygen site for each WO_4 tetrahedron. This terminal, or unconstrained [8], oxygen creates a structural openness along the high-symmetry $\langle 111 \rangle$ axes and is thought to be influential in the low-energy dynamics and crucial to the phenomenon of NTE in ZrW_2O_8.

Thermal expansion phenomena generally come from anharmonic phonon dynamics [1,6–10]. For ZrW_2O_8 analysis of temperature dependence [7–10] indicates that the low-energy region should be of primary importance. To probe the low-energy phonon dynamics we use temperature dependent infrared spectroscopy covering the range from 5000 to 16 cm^{-1} (600–2 meV), which encompasses all the optic phonons of ZrW_2O_8. We find that the phonon-related peaks in the infrared spectra extend to unusually low-energy ($\sim$3 meV) and that there is strong and unusual temperature dependence in the low-energy region, reflecting evidence of unconventional and anharmonic behavior. We suggest that understanding the mechanism of NTE and understanding the exotic nature of the infrared spectra from ZrW_2O_8 are two essentially similar problems, both rooted in exotic low-energy dynamics.

One of the central unresolved issues for ZrW_2O_8 has to do with the nature of the eigenmode(s) responsible for NTE. While earlier work has emphasized the role of transverse oxygen vibration [4–9] for the mechanism of NTE, Cao *et al.* [11,12] have proposed a model, based on x-ray absorption fine structure (XAFS) data, in which translation of WO_4 tetrahedra along $\langle 111 \rangle$ directions plays an important role. Using eigenvector calculations together with our data, we infer that transverse oxygen motion, in the form of libration, tends to be accompanied by translation within each low-energy mode (thus they are essentially inseparable). This mixing arises due to the unconstrained oxygen and the associated openness of the structure along the high-symmmetry $\langle 111 \rangle$ direction axes, and it appears to be essential to the nature of the low-frequency IR spectra. This mixing may also be crucial to the mechanism of the NTE: while the transverse oxygen motion provides the thermal motion that contracts the lattice, the presence of a translational component in each low-energy mode provides a source of frustration that inhibits lattice instabilities that would destroy NTE.

The single-crystal samples are grown using a layered self-flux technique [13]. Our measurements of the specular reflectivity cover the frequency range from 15 to 5000 cm^{-1} and the temperature range 20 to 300 K. The optical conductivity, $\sigma(\omega)$, is determined from the reflectivity via a Kramers-Kronig transform with carefully chosen upper and lower terminations. For the acentric $P2_13$ structure of ZrW_2O_8 one expects a total of 132 modes: 3 acoustic modes, 32 triplets of IR optical phonons, 11 doublets, and 11 singlets, associated with the irreducible representations $33T + 11E + 11A$ [14–16]. Our results are broadly consistent with earlier work

[14–18] for the higher frequency parts of the phonon spectrum, and complementary in our emphasis on the low-frequency range.

Figure 1(a) shows the real part of the optical conductivity, $\sigma_1(\omega)$, vs frequency. The infrared active optical phonon modes, which generally appear as peaks in $\sigma_1(\omega)$, are sufficiently dense that they tend to merge together into clusters in ZrW_2O_8. The upper cluster is associated with bond stretching motion (including the ν_3 modes of the WO_4 tetrahedra) and the middle cluster (180–400 cm^{-1}) with bond bending modes (e.g., ν_2 modes). Below these two clusters there are additional infrared features, shown in the inset, which we associate with librational and translational motion of WO_4 tetrahedra, as discussed below. Unlike the generic modes of the upper clusters, the modes in this region are specific to the ZrW_2O_8 structure, and it is in this lower region that one expects to find modes relevant to the mechanism of NTE.

As shown in Figs. 1(b) and 1(c), the peaks in this region extend to unusually low energy and exhibit striking temperature dependence. They tend to sharpen and grow in strength as the sample is cooled; they exhibit swept, asymmetric line shapes, and in some cases substantial dependence of peak frequency on temperature. The largest peak frequency shifts are observed for the broad 28 cm^{-1} mode, which shifts from about 27 to 29.5 cm^{-1} (+8%), and the 88 cm^{-1} mode, which shifts from about 91.5 to 86 cm^{-1} (−6%). These shifts are unusually large and the substantial accretion of spectral weight (presumably coming from the higher frequency) is beyond the scope of conventional phonon models. The pervasiveness of strong temperature dependence throughout this low-frequency region reflects the exotic character of the low-energy dynamics which is clearly evident in the IR spectra.

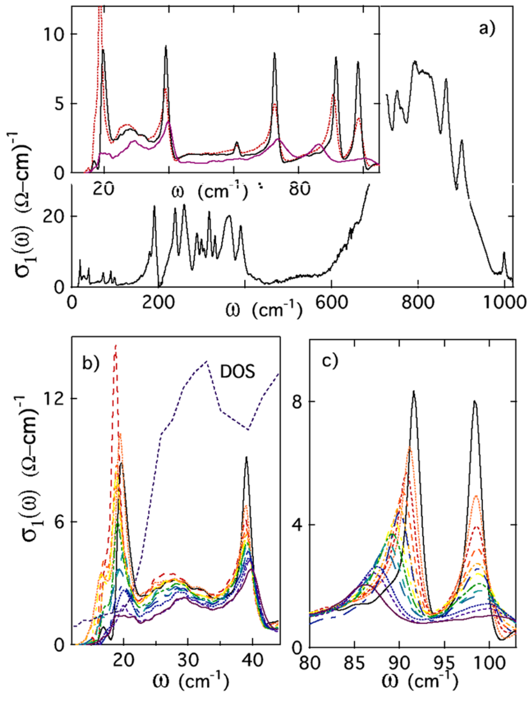

FIG. 1 (color online). (a) The real part of the conductivity, $\sigma_1(\omega)$, is shown for the entire optic phonon region. The inset shows the low-frequency region for temperatures of 20, 80 (dotted line), and 240 K. (b) and (c) show $\sigma_1(\omega)$ for $T = 20$, 60, 80, 100, 120, 140, 160, 180, 200, 220, 240, 260, and 300 K in two low ω regions, along with neutron density of states in (b) [8].

It is informative to consider the relationship between our IR data and specific heat [7]. For the fit shown in Fig. 2(a), a lowest energy Einstein mode at 28.5 cm^{-1} with a spectral weight of 2.6 oscillators per unit cell provides a good fit to the leading edge of $C(T)/T^3$ [19]. This fit is highly constraining with regard to the energy of the lowest Einstein mode; attempts to fit $C(T)$ with a lower optical mode generate excess specific heat at low temperature as shown in Fig. 2(a). We therefore conclude that the 20 cm^{-1} peak does not correspond to the zone-center end point of an ordinary optical phonon branch and that the broad 28 cm^{-1} peak is the signature of the lowest optical phonon of ZrW_2O_8. The total spectral weight in the peaks between 28 and 100 cm^{-1} is in agreement with the results of our phonon eigenvector calculations, discussed below, and the peaks in this region are in reasonable correspondence with zone-center intercepts of optical phonon dispersion relations calculated for the isostructural compound HfW_2O_8 [20,21] as well as neutron density of states (DOS) peaks [8]. The 20 cm^{-1} peak differs from the others in that it diminishes substantially below 80 K (the others grow) and is not reconcilable with neutron DOS and $C(T)$. These two features may suggest a low-density defect with an extremely large dipole matrix element. Further theory is needed, in conjunction with controlled defect studies, to ascertain the origin of this marked absorption, and its possible connection with the unusual lattice dynamics of the bulk compound.

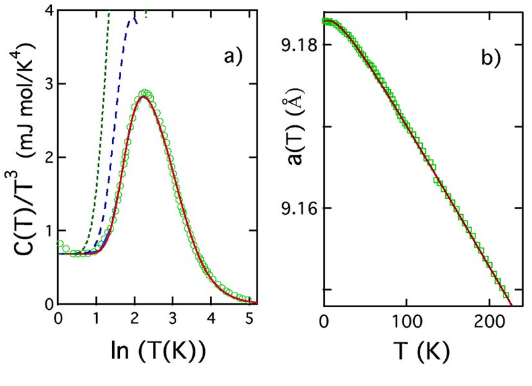

FIG. 2 (color online). (a) A fit to the specific heat with a lowest infrared mode at 28.5 cm^{-1} (3.5 meV) is shown by the solid line (through the specific heat data). The dashed curves show the excess specific heat generated by failed attempts to fit $C(T)$ with a lowest optic mode at 20 or 24 cm^{-1}, respectively. (b) $a(T)$ data (open squares) are shown along with a fit based on a two Einstein mode model.

Focusing on energetics, one can let the infrared spectra provide a context in which to explore the origins of the temperature dependence of the lattice parameter, $a(T)$. Similar to earlier work [8,9], we approach this by associating negative Grüneisen parameters (γ) with Einstein mode frequencies. We calculate $a(T)$ using a bulk modulus of 72 GPa [22] and assuming triplet weight [1]. Starting with the frequency of the lowest optic mode from our data (at 28 $\mathrm{cm}^{-1} = 3.5$ meV), we find that associating a large negative Grüneisen parameter to this mode alone does not allow a good fit to $a(T)$; however, a good fit can be obtained simply by including a second Einstein mode at higher frequency, as shown in Fig. 2(b) for $\gamma = -20$ at 28 cm^{-1} and $\gamma = -7$ at 88 cm^{-1}. The lower energy corresponds to the lowest energy optical phonon in ZrW_2O_8, which is so low it cuts through the acoustic phonon dispersion and may thereby acquire mixed character [21]; the higher energy corresponds to the strongly temperature dependent peak near 88 cm^{-1} [Fig. 1(c)]. While this two-mode approach provides the minimal context in which a good fit can be obtained, one can also do more nuanced fits involving additional modes. One can use Grüneisen parameters for modes above 40 cm^{-1} from pressure dependent Raman measurements of Ravindran *et al.* [16] and add an additional term for the 28 cm^{-1} mode. In that more nuanced approach good fits to $a(T)$ can be obtained when the γ's of the two lowest optic modes add to about -20.

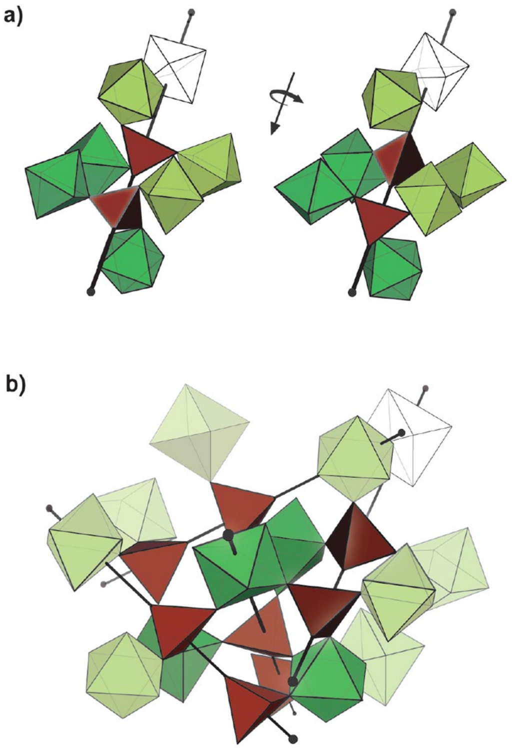

FIG. 3 (color online). (a) The nature of a low-frequency triplet mode is shown in terms of WO_4 tetrahedra and Zr-centered octahedra via a time sequence. As the tetrahedra rotate clockwise, they translate downward along the ⟨111⟩ axis, which is shown by the dark line. The two lowest-frequency optic modes are similar, but in the other one the ⟨111⟩ axis octahedron (white) rotates opposite the tetrahedra. The unconstrained oxygen lies on the ⟨111⟩ axis. (b) The pair of tetrahedra shown in (a) couples to other tetrahedra as shown. There are eight WO_4 tetrahedra in a unit cell organized in pairs on ⟨111⟩ axes (dark lines) which are offset in a spiral-staircase configuration as shown. (Illustration by Alison Kendall)

Mechanisms of NTE based on transverse thermal motion of oxygens in twofold coordination (W-O-Zr) have been widely considered [3–9]; however, Cao *et al.* [11,12] have proposed an alternative model, based on XAFS data, in which translation of WO_4 tetrahedra along the high-symmetry ⟨111⟩ axes plays a key role. Ultimately the discussion of mechanism centers on the eigenvectors of the relevant phonon modes. Toward this end, we have calculated the eigenvector for each $\mathbf{k} = 0$ optical phonon mode using a mass-spring model of a 44 atom unit cell [23] with nearest-neighbor stretching and bending interactions and periodic boundary conditions. With appropriate bond strengths, the eigenvectors exhibiting bond stretching and bending motion are associated with high (700–900 cm^{-1}) and moderate (150–400 cm^{-1}) frequency eigenvalues, respectively, as expected. For the range below about 120 cm^{-1} our calculation generates 27 additional optic modes, of which 21 are associated with triplets. The two lowest energy modes are triplets at 32 and 43 cm^{-1}, respectively, in reasonable correspondence with the data. The eigenvectors for these modes exhibit a mixture of librational and translational motion, as illustrated in Fig. 3(a). A suitable choice of eigenvector within the triplet degeneracy manifold is required to clarify the motion in this way. For the mode shown, clockwise rotation about the ⟨111⟩ axis is accompanied by downward translation of the two tetrahedra along the ⟨111⟩ axis [24]

This ⟨111⟩ axis pair is connected, via Zr-centered octahedra, to other tetrahedra as illustrated in Fig. 3(b). The are a total of eight WO_4 tetrahedra per unit cell arranged in pairs along ⟨111⟩ axes and offset from each other in a "spiral-staircase" pattern as shown. Motion on the other ⟨111⟩ is not the same [25] and the motions are correlated in complex ways.

This mixing of translational and rotational (librational) motion is intimately related to the underconstrained nature of the ZrW_2O_8 structure, in which each tetrahedron has an unconnected (terminal) oxygen at its ⟨111⟩ axis apex [7]. Because there are no strong second bonds for this unconstrained oxygen, translations of WO_4 tetrahedra along ⟨111⟩ axes do not involve significant bond compression and therefore project to very low frequency. There they tend to mix with the low-frequency librational motion, and it is through this mixing that these low-energy modes can acquire a dynamic dipole moment (since the WO_4 tetrahedra carry net charge). Our observation of nonzero dipole moment for many low-energy modes indicates that this mixing is pervasive. Thus the richness of the low-frequency infrared spectra is connected to the existence of the unconstrained oxygen and the related openness along the high-symmetry $\langle 111\rangle$ directions, which is a defining feature of the ZrW_2O_8 structure and critical to NTE [7–10,26].

Regarding the origins of anharmonicity in ZrW_2O_8, we note that, in the context of a simple harmonic picture, the uncertainties in the circumferential oxygen position would be substantial. Using the frequency of the lowest optic mode (28 cm^{-1}) one gets a theoretical uncertainty in the ground state of $\Delta\theta = \sqrt{2\hbar/m_o r^2\omega} \simeq 14°$ with a corresponding circumferential uncertainty $\Delta(r\theta) \simeq 0.4$ Å. These increase to about 40° and 1.2 Å by room temperature. Such large values suggest a possible origin of anharmonicity and motivate consideration of the relevance of configurational tunneling or rotation to the low-energy dynamics. Tunneling, rotation, and configurational exchange phenomenon have been observed in systems with a similar threefold rotation axis involving methyl-group tetrahedra [27,28], where the breakdown of the harmonic approximation for low-energy librational motion has been carefully studied. For methyl-group tetrahedra such as CH_3I the lowest librational mode frequency is typically 80 cm^{-1}, about 3 times higher than ZrW_2O_8. That most of this difference can be accounted for by the hydrogen-oxygen mass difference suggests a roughly comparable confining potential to lowest order. A possible difference between $X CH_3$ and WO_4 tetrahedra arises from the nuclear spin, which is $\frac{1}{2}$ for H and 0 for the O^{16} nucleus; therefore a 120° reorientation of a WO_4 tetrahedron is equivalent to a double permutation among identical particles and thus does not produce a distinct state. The potential relevance of finite barrier phenomena and large oxygen excursions to the low-energy dynamics of ZrW_2O_8 remains a question for future work.

We have provided evidence for highly unusual low-energy phonon dynamics in ZrW_2O_8 as reflected in our infrared spectra. We infer that the lowest optic modes in ZrW_2O_8 tend to have a mixed librational and translational character in which the unconstrained oxygen plays an essential role, and it is likely that these modes play a central role in the mechanism of negative thermal expansion. While further work is needed to fully elucidate the mechanism of NTE in ZrW_2O_8, the present work shows that both librational and translational motions are operative: the transverse oxygen motion associated with libration provides NTE, while the translational component within each mode frustrates a displacive transition that would otherwise remove the unique structural environment in which these mixed phonon modes exist.

We gratefully acknowledge F. Bridges, D. Cao, O. Narayan, and W. E. Pickett for helpful conversations. This work done at UCSC was supported by NSF Grant No. DMR-0071949.

[1] N.W. Ashcroft and N. D. Mermin, *Solid State Physics* (Saunders College, Philadelphia, 1976).
[2] G. K. White, Contemp. Phys. **34**, 193 (1993).
[3] A.W. Sleight, Curr. Opin. Solid State Mater. Sci. **3**, 128 (1998).
[4] T. A. Mary, J. S. O. Evans, T. Vogt, and A.W. Sleight, Science **272**, 90 (1996).
[5] J. S. O. Evans, T. A. Mary, T. Vogt, M. Subramanian, and A.W. Sleight, Chem. Mater. **8**, 2809 (1996).
[6] A. K. A. Pryde, K. D. Hammonds, M.T. Dove, V. Heine, J. D. Gale, and M. C. Warren, J. Phys. Condens. Matter **8**, 10973 (1996).
[7] A. P. Ramirez and G.R. Kowach, Phys. Rev. Lett. **80**, 4903 (1998).
[8] G. Ernst, C. Broholm, G. R. Kowach, and A. P. Ramirez, Nature (London) **396**, 147 (1998).
[9] W. I. F. David, J. S. O. Evans, and A.W. Sleight, Europhys. Lett. **46**, 661 (1999).
[10] R. Mittal and S. L. Chaplot, Phys. Rev. B **60**, 7234 (1999).
[11] D. Cao, F. Bridges, G. R. Kowach, and A. P. Ramirez, Phys. Rev. Lett. **89**, 215902 (2002).
[12] D. Cao, F. Bridges, G. R. Kowach, and A. P. Ramirez, Phys. Rev. B **68**, 14303 (2003).
[13] G. R. Kowach, J. Cryst. Growth **212**, 167 (2000).
[14] T. R. Ravindran, A. K. Arora, and T. A. Mary, Phys. Rev. Lett. **84**, 3879 (2000).
[15] B. Chen, D.V. S. Muthu, Z. X. Liu, A.W. Sleight, and M. B. Kruger, Phys. Rev. B **64**, 214111 (2001).
[16] T. R. Ravindran, A. K. Arora, and T. A. Mary, J. Phys. Condens. Matter **13**, 11573 (2001).
[17] Y. Yamamura, N. Nakajima, T. Tsuji, M. Koyano, Y. Iwasa, S. Katayama, K. Saito, and M. Sorai, Phys. Rev. B **66**, 014301 (2002).
[18] T. R. Ravindran, A. K. Arora, and T. A. Mary, Phys. Rev. B **67**, 64301 (2003).
[19] The fit includes a $\Theta_D = 62$ cm^{-1} and Einstein contributions at IR and Raman peak frequencies above 28 cm^{-1}.
[20] R. Mittal, S. L. Chaplot, H. Schober, and T. A. Mary, Phys. Rev. Lett. **86**, 4692 (2001).
[21] R. Mittal, S. L. Chaplot, A. I. Kolesnikov, C. K. Loong, and T. A. Mary, Phys. Rev. B **68**, 54302 (2003).
[22] J. D. Jorgensen, Z. Hu, S. Teslic, D. N. Argyriou, S. Short, J. S. O. Evans, and A.W. Sleight, Phys. Rev. B **59**, 215 (1999).
[23] M. Auray, M. Quarton, and M. LeBlanc, Acta Crystallogr. Sect. C **51**, 2210 (1995).
[24] For most parameter choices, this is one of the two lowest energy modes. In the other, the $\langle 111\rangle$-axis octahedra rotates opposite to the two tetrahedra. Two singlet modes with purely translational motion (along the $\langle 111\rangle$ axes) also occur at relatively low frequencies which are sensitive to weak next-nearest-neighbor interactions.
[25] The motion includes librations in which the unconstrained oxygens tilt away from their $\langle 111\rangle$ axes.
[26] S. Allen and J. S. O. Evans, Phys. Rev. B **68**, 134101 (2003).
[27] M. Prager and A. Heidemann, Chem. Rev. **97**, 2933 (1997).
[28] R. M. Dimeo, Am. J. Phys. **71**, 885 (2002).